J. S. Afr. Inst. Min. Metall., vol. 91, no. 5.
May 1991. pp. 145-157.

Energy changes in a rockmass containing multiple discontinuities

by J.A.L. NAPIER*

SYNOPSIS

Many tabular mining problems can be modelled effectively by displacement-discontinuity techniques, which can be extended directly to represent fracturing on discrete planes and movements on planes of weakness. This paper presents a unified method for computing the energy changes that occur when multiple discontinuities intersect and are extended incrementally. It shows how this method can be used to deduce energy-release information for standard layout problems and, in addition, how the technique can be incorporated in numerical procedures based on the displacement-discontinuity method. Examples are given to demonstrate the effects of off-reef fracturing and the importance of stope–fault intersections during seismic events.

SAMEVATTING

Baie tafelmynbouprobleme kan doeltreffend gemodelleer word met verplasingsdiskontinuïteitstegnieke wat regstreeks uitgebrei kan word om breukvorming op afsonderlike vlakke en bewegings op swak vlakke voor te stel. Hierdie referaat bied 'n saambindende metode vir die berekening van die energieveranderinge wat plaasvind wanneer meervoudige diskontinuïteite mekaar kruis en inkrementeel verleng word. Dit toon hoe hierdie metode gebruik kan word om inligting oor energievrystelling vir standaarduitlegprobleme op te lei, en verder hoe die tegniek ingesluit kan word by numeriese prosedures wat op die verplasingsdiskontinuïteitmetode gebaseer is. Daar word voorbeelde gegee om die uitwerking van breukvorming van die rif af en die belangrikheid van kruisings tussen afbouplekke en verskuiwings tydens seismiese gebeurtenisse te demonstreer.

Introduction

Displacement discontinuities or dislocations are a functionally useful means of representing features such as mining-induced fractures, parting planes, joints and weak fault planes interspersed throughout an otherwise intact rock mass. Displacement discontinuities have also been used to model extensive, flat mining excavations in which the mining width is negligible in comparison with the areal extent of the excavations. If a sufficient number of discontinuities are used, it is possible to simulate the zone of fracture surrounding tabular stopes in brittle rock as an elastic problem in which the elastic body is bounded by an external surface and by an extended set of internal surfaces that correspond to each side of the imbedded discontinuity surfaces. All inelastic or non-linear behaviour is localized at the discontinuity interfaces.

This paper presents basic derivations of the energy changes that arise in an elastic medium containing multiple discontinuities. These results are illustrated by analyses of the energy release that occurs when both tabular excavations and fracture surfaces are extended. The implementation of energy-change computations in computer codes is discussed, and the numerical analysis of energy release associated with the intersection of a fault plane and a stope, and a simulation of stope face fracturing, are presented.

Special forms of the results presented in this paper have been given previously by Salamon[1-3] and Walsh[4] for tabular excavations, by Savage and Walsh[5] and Aki and Richards[6] for the analysis of slip on a fault, and by Piper and Ryder[7] for the estimation of the energy release associated with some fill-rib and strip-pillar mine layouts. It is demonstrated in this paper that the fundamental results derived by Salamon for tabular excavations can be applied to a general class of problems involving multiple interacting and intersecting discontinuities in an elastic medium.

* Chamber of Mines Research Organization, P.O. Box 91230, Auckland Park, 2006 Transvaal

© The South African Institute of Mining and Metallurgy, 1991. SA ISSN 0038-223X/3.00 + 0.00. Paper received 14th March, 1990.

Fundamental Energy Relationships

Conceptual Model of Energy Changes

The computation of the energy changes that accompany mining activity requires specific assumptions concerning the excavation sequence and the representation of failure and fracturing in the rockmass. In the present analysis, it is assumed that the excavations are tabular and can be represented by zero width 'slits' or 'cuts' in the medium. As mining proceeds, these dislocation surfaces are progressively enlarged, but no material is removed from the system. It is also assumed that failure in the material is localized on fracture surfaces that are again represented by cuts in the medium. This implies that the displacement field is continuous everywhere except at the discontinuity interfaces, where it will undergo a 'jump' or 'displacement discontinuity' across the interface.

A further assumption is now made that the rockmass is perfectly elastic. A thermodynamic system can then be defined to comprise a region of elastic material bounded by an external surface and internal surfaces corresponding to each side of the discontinuities in the medium. The energy changes that occur as the discontinuity surfaces are extended in discrete steps can be accounted for, in principle, if the surface tractions and the discontinuity jumps are known at each step. This process can include the addition of fracture surfaces at critical positions to represent failure in the intact rockmass as mining continues.

In the analysis of this system, the external bounding surface is assumed to be fixed or to have fixed tractions imposed upon it. It is also noted that fixed body forces will act at each point in the medium. When relative movement occurs at the discontinuity interfaces, these fixed forces will be displaced and will perform work on the body. The evolution between the initial and the final states is assumed to occur by making a series of step-wise changes to the tractions on the discontinuity interfaces. It should be noted that all the discontinuities can be assumed to be present in the initial state with suitable holding tractions imposed on those discontinuities which are not mobilized. The energy changes that accompany the step-wise alteration of tractions at each step will depend on the mechanical processes occurring at the interfaces, and on the manner in which the holding tractions are altered. In general, the rockmass will perform accountable work in deforming artificial support or in sliding against friction. However, the kinetic energy that may be generated as the holding tractions are suddenly altered cannot be directly accounted for in a static analysis. The unaccounted energy should be positive in each step for a given sequence of evolutionary changes to be feasible as a spontaneous process. The unaccounted energy can therefore be considered to be a measure of the 'driving' energy that is available for each successive step. It is also important to note that the equilibrium position that is estimated in a static analysis of incremental steps may not coincide with the actual position, which is attained after a sudden change in the holding tractions during any step. This discrepancy is assumed to be small.

Energy Balance Equations

Consider a thermodynamic 'system' comprising a volume, V, of elastic rock that is bounded by an external surface, S_e, and by internal discontinuity surfaces having two sides, S_d^+ and S_d^-, that separate the elastic material on each side of the discontinuities. (See the Addendum.) The total surface area of the body can be expressed as

$$S = S_e + S_d^+ + S_d^- \quad \ldots\ldots (1)$$

It is assumed that the rockmass is in a primitive state p, which is in equilibrium. A change in this state is then effected by alteration of the boundary tractions that are applied to the discontinuity surfaces. The new equilibrium state that is reached when all motions have ceased is denoted by t, and it is assumed that no net thermal energy is added to the system. The energy changes occurring between state p and state t can be described by the first law of thermodynamics in the following form (see, for example, Malvern[8]):

$$\Delta Q' + \Delta W' = \Delta E, \quad \ldots\ldots (2)$$

where $\Delta Q'$ = incremental heat energy supplied to the system
$\Delta W'$ = incremental work done on the system
ΔE = change in internal energy.

By assumption that no net thermal energy is added to the system, $\Delta Q' = 0$. The term $\Delta W'$ in equation (2) represents the work done on the system by body forces and surface tractions in bringing the rockmass to the new state of equilibrium, t. It is convenient to partition $\Delta W'$ into two terms, ΔW and ΔW_D, such that

$$\Delta W' = \Delta W - \Delta W_D. \quad \ldots\ldots (3)$$

The first term, ΔW, represents the incremental work done on the rockmass by fixed body forces and by any fixed tractions specified on the external surface, S_e. The second term, ΔW_D, denotes the incremental work that is done against the equilibrium reaction forces acting at the discontinuity interfaces. These arise from reactions generated by artificial support or from the resistance to sliding against friction.

In the change to the new state, it is assumed that any kinetic energy that is generated will be dissipated eventually, increasing the internal energy of the body. In addition to this, the contribution of the elastic strain energy to the internal energy of the rockmass will be altered. The total change in internal energy, ΔE, can be written as

$$\Delta E = \Delta W_R + \Delta U, \quad \ldots\ldots (4)$$

where ΔW_R = kinetic energy dissipated in changing from state p to state t
ΔU = changes in elastic strain energy between state p and state t.

Substitution from equations (3) and (4) into equation (2) yields

$$\Delta W_R = \Delta W - \Delta U - \Delta W_D. \quad \ldots\ldots (5)$$

It is convenient to define the difference between the incremental work done on the system by fixed forces, ΔW, and the incremental strain energy change, ΔU, as the 'available' energy, ΔW_A. Therefore, the substitution of

$$\Delta W_A = \Delta W - \Delta U \quad \ldots\ldots (6)$$

into equation (5) yields the following expression for the component of kinetic energy that is dissipated:

$$\Delta W_R = \Delta W_A - \Delta W_D. \quad \ldots\ldots (7)$$

It is shown in the Addendum that the increment in available energy, ΔW_A, depends only on the changes in tractions and displacement discontinuities at the discontinuity surfaces, S_d, between state p and state t. The dissipated energy increment, ΔW_D, depends on the constitutive properties of the discontinuity interface, including the work absorbed in deforming support, compressing backfill, and sliding against friction. ΔW_D may also include energy absorbed in the creation of new discontinuity surfaces during rupture, but this is not considered here.

It is understood that all incremental expressions such as ΔW_A are to be interpreted as $\Delta W_A = W_A^t - W_A^p$, where the quantities W_A^t and W_A^p represent the total increment between an initial 'virgin' state, v, and the states t or p respectively. Expressions for the incremental changes ΔW, ΔU, and ΔW_A are derived in the Addendum, and are summarized in Table I. The particular expressions that obtain when the primitive state p is actually the virgin state v are also included in Table I. The expressions in Table I are in terms of traction vector components, T_i^q, and components of the displacement jumps, $D_i^q = u_i^{q-} - u_i^{q+}$, which exist on the discontinuity surfaces S_d in state q, where q corresponds to v,

TABLE I
EXPRESSIONS FOR TOTAL AND INCREMENTAL CHANGES IN ENERGY

Quantity	Total change	Incremental change
Energy supplied	$W^t - U^v = -\int_{S_d} T_i^v D_i^t \, dS$	$\Delta W = \int_{S_d} (T_i^t D_i^p - T_i^p D_i^t) \, dS$
Strain energy	$U^t - U^v = \frac{1}{2}\int_{S_d} (T_i^t - T_i^v) D_i^t \, dS$	$\Delta U = \frac{1}{2}\int_{S_d} (T_i^t - T_i^p)(D_i^t - D_i^p) \, dS$
Available energy	$W_A^t - W_A^v = -\frac{1}{2}\int_{S_d} (T_i^t + T_i^v) D_i^t \, dS$	$\Delta W_A = -\frac{1}{2}\int_{S_d} (T_i^t + T_i^p)(D_i^t - D_i^p) \, dS$

p, or t as indicated. The key result in Table I is the expression for the increment in available energy given by

$$\Delta W_A = -\tfrac{1}{2}\int_{S_d} (T_i^p + T_i^t)(D_i^t - D_i^p) \, dS. \quad \ldots\ldots (8)$$

In equation (8), repeated indices are assumed to be summed over the component range of the vector quantities, for example, $T_i^p D_i^t = T_x^p D_x^t + T_y^p D_y^t + T_z^p D_z^t$ where x, y, z form a local axis system at the discontinuity surface. Equation (8) is essentially the result referred to by Aki and Richards[6] as the 'Volterra relation'.

As noted in the Addendum, the incremental change in the available energy can also be obtained by computation of the difference between the total available energy in the final state, W_A^t, and the total available energy in the primitive state, W_A^p. Explicitly,

$$W_A^p = -\tfrac{1}{2}\int_{S_d} (T_i^v + T_i^p) D_i^p \, dS \quad \ldots\ldots (9)$$

and

$$W_A^t = -\tfrac{1}{2}\int_{S_d} (T_i^v + T_i^t) D_i^t dS. \quad \ldots\ldots (10)$$

In certain cases, it is more convenient to determine the difference $W_A^t - W_A^p$ as given by equations (9) and (10) than to evaluate ΔW_A direct from equation (8). This is illustrated later.

Mechanisms of Energy Dissipation

The term ΔW_D in equation (3) represents the work dissipated by reaction forces at the discontinuity interfaces. This is considered to be the work done in compressing artificial support in stopes, or the work done against frictional resistance at a sliding interface.

The work done by the rockmass on artificial support depends on the specific form of the support reaction as a function of the support strain. The support strain can be expressed conveniently in terms of the excavation closure that is represented by the normal component, D_n, of the displacement jump between the roof and the floor of the excavation. This is illustrated in Fig. 1 for a backfill material placed in a stope of initial width, h. In this case, the stope is required to close by an amount D_n° before a reaction stress is generated by the fill material.

In Fig. 1, D_n^t represents the equilibrium closure and R_n^t the corresponding absolute support reaction stress. The work done on the support over an area A of the discontinuity surface can be written in the form,

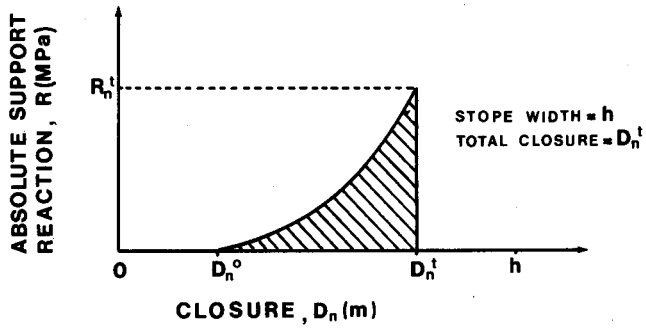

Fig. 1—Support reaction as a function of tabular excavation closure

$$\Delta W_D = f R_n^t D_n^t A, \quad \ldots\ldots (11)$$

where f represents the ratio of the shaded area in Fig. 1 to the total area $R_n^t \times D_n^t$. In the particular case where fill material is introduced at the stoping width h, f can be related to the 'figure of merit' parameter M[2,7] by the relation

$$f = 1 - M. \quad \ldots\ldots (12)$$

The work done against friction at a discontinuity interface depends on the loading and surface characteristics of the sliding discontinuities. Resistance to sliding is generally a function of the amount of slip and of the normal stress acting across the discontinuity. If it is assumed that the shear slip (ride) on a discontinuity is D_s, and that the dilation, D_n, is proportional to the slip, then

$$D_n = -\tan\psi |D_s|, \quad \ldots\ldots (13)$$

where ψ is the angle of dilation. The total shear resistance to slip must be determined according to a specific conceptual model of the dilation mechanism. If a simple ramp mechanism is postulated, it can be shown that the work absorbed by frictional sliding over an area A of the joint surface is

$$\Delta W_D = T_n[\tan(\phi + \psi) - \tan(\psi)] |D_s| A, \quad \ldots\ldots (14)$$

where T_n represents the total normal stress to the surface and D_s represents an incremental amount of slip. In a static analysis, the relationship between T_n and D_s is not known explicitly over the step. It is assumed here that T_n is equal to the final stress, T_n^t, in each step.

The energy dissipated by support and friction sliding is found by the integration of equation (11) or (14) over the discontinuity surfaces at each step of a sequence of incremental changes. The sum of the energies dissipated will, in general, depend on the particular sequence chosen.

Energy Changes Associated with Small Mining Steps

Salamon[1,3] has expressed the fundamental energy balance for the enlargement of openings in an elastic medium in the following form:

$$W_r = (W + U_m) - (U_c + W_s), \quad \ldots\ldots\ldots\ldots (15)$$

where

W_r = unaccounted energy released in reaching the new equilibrium state
W = work done by external and body forces
U_m = strain energy released from the removed material
U_c = strain-energy change in the remaining material
W_s = work done in deforming support.

Salamon has demonstrated that, if the excavation is made in small steps, the external work, W, tends to $U_c + W_s$. The unaccounted energy, W_r, therefore approaches the strain energy, U_m, released from the excavated material, and mining in small steps is inferred to be an aseismic process in an unfractured elastic medium.

A comparison of equations (15) and (5) shows that ΔU in equation (5) is equivalent to $U_c - U_m$ and is the net change in strain energy of the whole system. In the present study, energy changes are associated with discontinuity surfaces and, since no material is actually removed, $U_m = 0$. Moreover, it is observed that, at great depth, the rock close to excavation surfaces can be extensively fractured and the strain energy, U_m, contained in mined increments will be small. The component of unaccounted energy, W_r, cannot then be inferred to be associated with the strain energy, U_m, of the mined material, and must be dissipated by an alternative mechanism that will not necessarily be aseismic. Specifically, if the removal of material from the mining face results in a small drop in the confinement of brittle material close to its failure limit, rapid load shedding can occur, which will not be immediately equilibrated by the surrounding material. This could, for example, be manifested as a 'face burst'.

It is particularly important to note that equation (8) represents the available energy, ΔW_A, that is to be dissipated following a mining step. The actual amount of energy that is dissipated, ΔW_D, and consequently the implied level of hazard associated with the unaccounted energy, ΔW_R, will depend on the specific geometric nature of the fracture zone and the failure processes that occur in this zone. The results derived in this paper are intended to facilitate explicit modelling of the fracture zone and the accompanying energy changes.

Implementation of Energy-change Computations in Stress-analysis Programs

The computation of the various energy quantities shown in Table I can be included without difficulty in stress-analysis programs based on the displacement-discontinuity method[9,10]. In this method, values of displacement discontinuity are determined in 'elements' covering the excavated areas. Integrals such as equation (8) can be evaluated directly by summing of the contribution from each element comprising the discontinuity surfaces. This procedure has been implemented in a special-purpose computer program, DIGS (Discontinuity Interaction and Growth Simulation).

Several case studies are discussed in this paper. However, it should be emphasized that the results in Table I are completely general for all types of discontinuity surfaces, allowing energy changes to be assessed for all problems involving interacting tabular excavations, and fracture and fault planes.

Application to Tabular Layouts

The application of the results in Table I to certain tabular layout geometries are illustrated here. Consider, for example, a rectangular excavation having a length L and a width X lying in a horizontal plane as shown in Fig. 2. The mining height, h, is presumed to be negligible compared with the dimension X or L. An approximate condition of plane strain will exist with respect to the axial direction, L, if L is much larger than the transverse dimension, X. The energy changes that result from extensions to the excavation in the direction X or L can be defined, respectively, as follows:

(i) Changes in 'transverse' energy occur when the long axis, L, is fixed and the excavation width is extended by an incremental distance, ΔX.
(ii) Changes in 'axial' energy occur when the excavation width, X, is fixed and the long axis, L, is extended by an incremental distance, ΔL.

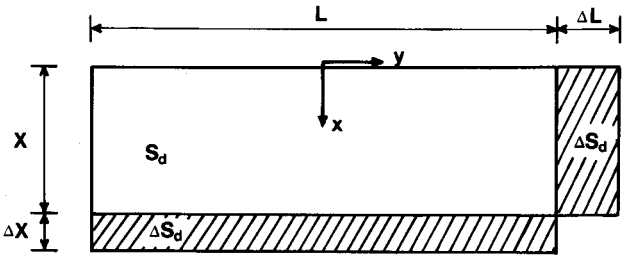

Fig. 2—Extension of a rectangular excavation in the axial direction, L, or transverse direction, X

Since the excavation is horizontal and in plane strain, the components of displacement discontinuity and of virgin traction are assumed to be given by

$$[D_i] = \begin{bmatrix} 0 \\ 0 \\ D_z(x) \end{bmatrix} \quad \ldots\ldots\ldots\ldots (16)$$

and

$$[T_i^v] = \begin{bmatrix} 0 \\ 0 \\ Q_z \end{bmatrix} \quad \ldots\ldots\ldots\ldots (17)$$

respectively, where the vertical closure component, $D_z(x)$, depends only on the transverse position, x, and the vertical virgin stress component, Q_z, is constant.

Changes in Transverse Energy

The incremental change in available energy, ΔW_A, that occurs when a change, ΔX, is made to the width of the excavation (shown in Fig. 2) can be most easily evaluated by determining the difference between W_A^p and W_A^t given by equations (9) and (10), respectively. For transverse extension to the excavation, the elementary surface area dS in these equations is replaced by $L\,dx$, where dx is an increment in the transverse direction. Consequently, using equations (16) and (17) and assuming that the excavation surfaces are unstressed, equations (9) and (10) become

$$W_A^p = -\tfrac{1}{2}L\,Q_z\int_0^X D_z^p(x)dx \quad \text{..... (18)}$$

and

$$W_A^t = -\tfrac{1}{2}L\,Q_z\int_0^{X+\Delta X} D_z^t(x)dx. \quad \text{..... (19)}$$

Since no energy is dissipated by support or frictional sliding, the release in transverse energy per unit area advanced is

$$ERR_T = (W_A^t - W_A^p)/L\cdot\Delta X. \quad \text{..... (20)}$$

For a parallel-sided panel of span s, it can be shown[11] that, if no total closure occurs,

$$\int_x^s D_z(x)dx = -[\pi(1-\nu^2)/2E]\,Q_z s^2, \quad \text{..... (21)}$$

where E is the Young's modulus and ν is the Poisson's ratio. When this result is used to evaluate equations (18) and (19), and W_A^p and W_A^t are substituted in equation (20), the transverse-energy release rate becomes

$$ERR_T = [\pi(1-\nu^2)\,Q_z^2/2E]\,[X + \Delta X/2]. \quad \text{..... (22)}$$

As ΔX becomes very small, this tends to

$$ERR_T = \pi(1-\nu^2)\,Q_z^2 X/2E. \quad \text{..... (23)}$$

If the transverse dimension, X, is very large, total closure will take place and the total traction components on the excavation will become equal to the virgin traction:

$$[T_i^p] = [T_i^t] = \begin{bmatrix} 0 \\ 0 \\ Q_z \end{bmatrix}. \quad \text{..... (24)}$$

If the vertical closure is set equal to the mining height, $D_z = h$, equations (9) and (10) become

$$W_A^p = -\tfrac{1}{2}(2Q_z)L\cdot X\cdot h \quad \text{..... (25)}$$

and

$$W_A^t = -\tfrac{1}{2}(2Q_z)L\cdot(X + \Delta X)\cdot h. \quad \text{..... (26)}$$

Substitution of these values of W_A^t and W_A^p into equation (20) gives

$$ERR_T = -Q_z h, \quad \text{..... (27)}$$

which is the well-known asymptotic rate of energy release for a parallel-sided panel with a very large span in which total closure has occurred[12].

If the span is very large and if backfill is present, the closure will be limited to D_z^t, and consequently, from equations (25) and (26),

$$\Delta W_A = W_A^t - W_A^p = -Q_z\cdot L\Delta X\cdot D_z^t. \quad \text{..... (28)}$$

The work adsorbed by the backfill is given by equation (11) with the fill reaction, R_n^t, replaced by $-Q_z$, and with the normal closure, D_n^t, replaced by D_z^t. These substitutions give

$$W_D^p = -f\cdot Q_z\cdot D_z^t\cdot L\cdot X. \quad \text{..... (29)}$$

and

$$W_D^t = -f\cdot Q_z\cdot D_z^t\cdot L\cdot(X + \Delta X). \quad \text{..... (30)}$$

The released or unaccounted energy is given by $\Delta W_R = \Delta W_A - \Delta W_D$, where $\Delta W_D = W_D^t - W_D^p$. The transverse-energy release rate per unit area of mining is therefore equal to

$$ERR_T = \Delta W_R/L\cdot\Delta X = -(1-f)Q_z D_z^t$$

or

$$ERR_T = -MQ_z D_z^t, \quad \text{..... (31)}$$

where M, given by equation (12), is the 'figure of merit'[7].

Changes in Axial Energy

In this case, the excavation shown in Fig. 2 is extended by an incremental distance ΔL in the direction of axis L. Employing equations (9) and (10) gives the total available energy change before and after the mining increment as

$$W_A^p = -\tfrac{1}{2}Q_z L\int_0^X D_z(x)dx \quad \text{..... (32)}$$

and

$$W_A^t = -\tfrac{1}{2}Q_z(L + \Delta L)\int_0^X D_z(x)dx. \quad \text{..... (33)}$$

The average axial-energy release rate per unit area over the width of the excavation, X, is given by

$$ERR_A = (W_A^t - W_A^p)/X\cdot\Delta L. \quad \text{..... (34)}$$

By substitution from equations (32) and (33) into (34),

$$ERR_A = -\tfrac{1}{2}Q_z\bar{D}_z, \quad \text{..... (35)}$$

where $\bar{D}_z$ represents the average closure over the width of the panel,

$$\bar{D}_z = (1/X)\int_0^X D_z(x)dx. \quad \text{..... (36)}$$

From equation (21), the average closure over a single parallel-sided panel of span X is

$$\bar{D}_z = -[\pi(1-\nu^2)/2E]\,Q_z X$$

and, consequently from equation (35),

$$ERR_A = \pi(1-\nu^2)\,Q_z^2 X/4E, \quad \text{..... (37)}$$

which is half the transverse-energy release rate given by equation (23).

For the case of an infinite train of similar panels of span s whose centres are spaced at intervals P with $P > s$, the integral of the closure over the panel width is given[11] by

$$N(s) = \int_0^s D_z(x)dx =$$

$$[4(1-\nu^2)\,Q_z/\pi E]\,P^2\,\log[\cos(\pi s/2P)]. \quad \text{..... (38)}$$

From this expression, the transverse-energy and average axial-energy release rates per panel can be deduced from equations (20) and (34) respectively in the form

$$ERR_T = -\tfrac{1}{2}Q_z \frac{\partial N}{\partial s} \quad \text{..... (39)}$$

and

$$ERR_A = -\tfrac{1}{2}Q_z\, N/s. \quad \text{..... (40)}$$

These results can be most usefully expressed as the ratio ERR_A/ERR_T, which is given by

$$\frac{ERR_A}{ERR_T} = \frac{-\log[\cos\Theta]}{\Theta \tan\Theta}, \quad \text{..... (41)}$$

where the angle Θ is expressed in terms of the extraction ratio $e = s/P$ in the form

$$\Theta = \frac{\Pi}{2}\left(\frac{s}{P}\right) = \frac{\Pi e}{2}. \quad \text{..... (42)}$$

In the special case where the panels become very far apart, $P \to \infty$ and $e \to 0$. It can be shown that $ERR_A/ERR_T \to 1/2$ in agreement with the results deduced for an isolated panel. The ratio given by equation (41) is shown in Fig. 3 as a function of the extraction ratio, e; for example, at an extraction ratio of 85 per cent, the average axial-energy release rate is slightly more than a quarter of the transverse-energy release rate.

Numerical Applications

If the analysis of bodies containing multiple cracks, including mine-layout problems, is carried out by the displacement-discontinuity method[9], the energy quantities introduced previously can be computed directly. In particular, the following three integrals can be routinely computed for specified portions of the discontinuity surfaces:

$$\Delta W = \int_{S_d} [T_i^t D_i^p - T_i^p D_i^t]\, dS \quad \text{..... (43)}$$

$$\Delta U = \tfrac{1}{2}\int_{S_d} [T_i^t - T_i^p][D_i^t + D_i^p]\, dS \quad \text{..... (44)}$$

$$\Delta W_A = -\tfrac{1}{2}\int_{S_d} [T_i^t + T_i^p][D_i^t - D_i^p]\, dS. \quad \text{..... (45)}$$

ΔW represents the incremental work done on the system, and ΔU represents the change in internal strain energy between state p and state t. Applications of these formulae are illustrated in the following sections. The integrals (43) to (45) have been implemented in a computer program DIGS, which uses linear variation of discontinuity strength in each element. In addition to the energy integrals, volumes of ride and closure are computed on all stope and fracture segments. Total changes in energy from the virgin state can also be computed from equations (43) to (45) by the setting of $T_i^p = T_i^v$ and $D_i^p = 0$.

Energy Release on a Fault

The energy released by slip on a fault plane can be evaluated by the application of equation (45) with the relevant tractions and displacement discontinuities that obtain before and after slip has occurred. In addition, the energy absorbed by friction sliding can be computed by the integration of equation (14) over the incremental area of slip.

In the special case where slip occurs in one tangential direction, s, the incremental ride, R, is defined as

$$R = D_s^t - D_s^p. \quad \text{..... (46)}$$

The excess shear stresses on the fault before and after slip are defined as, respectively,

$$\tau_e^p = |T_s^p| + \mu T_n^p \quad \text{..... (47)}$$

and

$$\tau_e^t = |T_s^t| + \mu T_n^t, \quad \text{..... (48)}$$

where T_n^p and T_n^t denote the traction components normal to the fault plane. (According to the sign convention used in this paper, these are assumed to be negative when compressive.) If the fault plane is denoted by F, the energy dissipated by sliding is given by

$$\Delta W_D = -\int_F \mu T_n^t |R| dS, \quad \text{..... (49)}$$

where it is assumed that the shear resistance is controlled by the final state of normal stress, T_n^t, which is compressive. This, in turn, implies that no opening occurs along the fault, and equation (45) becomes

$$\Delta W_A = -\tfrac{1}{2}\int_F (T_s^t + T_s^p)\, R\, dS. \quad \text{..... (50)}$$

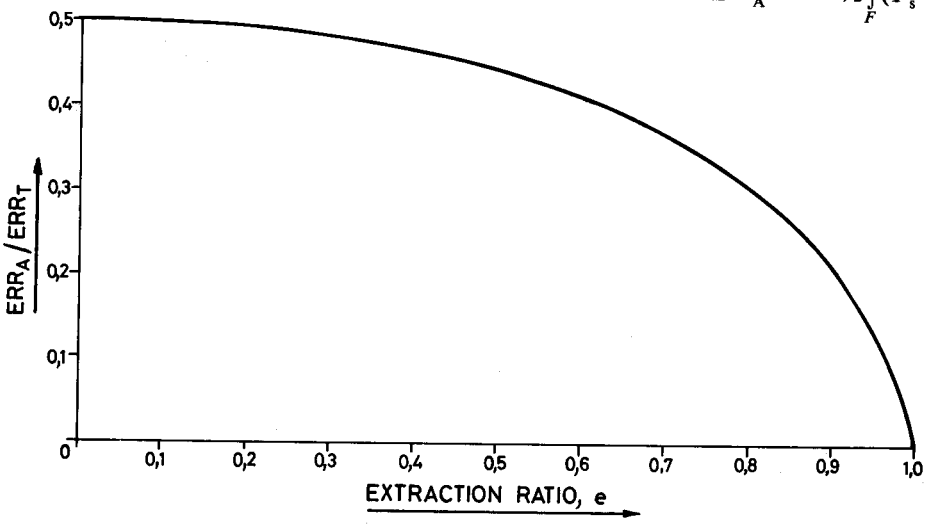

Fig. 3—Ratio of the axial-energy release rate to the transverse-energy release rate for an infinite train of parallel-sided panels

It is apparent that, if slip is initiated, the sign[6] of the shear stress, T_s^p, and the ride, R, will be opposite. Equation (50) can therefore be written as

$$\Delta W_A = \tfrac{1}{2}\int_F (|T_s^t| + |T_s^p|)|R|dS. \quad \ldots\ldots (51)$$

Substitution of the absolute shear stresses implied by equations (47) and (48) into (51) and subtraction of the work dissipated by friction, equation (49), gives the net energy released in the form

$$\Delta W_R = \tfrac{1}{2}\int_F [\tau_e^p + \mu(T_n^t - T_n^p)]|R|dS, \quad \ldots\ldots (52)$$

where it has been assumed that the condition for static equilibrium in the final state is $\tau_e^t = 0$.

In the special case where the normal stress across the fault does not change after slip has occurred, $T_n^t = T_n^p$ and equation (52) becomes identical to the expression given by Ryder[13] for the energy released on a fault. Alternatively, by replacing T_n^t in equation (49) with an average normal stress defined as

$$T_n = \tfrac{1}{2}(T_n^p + T_n^t) \quad \ldots\ldots (53)$$

and by subtracting equation (49) from (51), equation (52) can be written as

$$\Delta W_R = \tfrac{1}{2}\int_F \tau_e^p |R|dS. \quad \ldots\ldots (54)$$

Since the normal stress across a fault will not necessarily remain fixed after slip has occurred, and since multiple components of the displacement-discontinuity vector may be mobilized, it is appropriate to use equation (45) for the determination of the change in available energy and an expression such as equation (49) for the work dissipated by friction, rather than restricted expressions such as (52) or (54).

To demonstrate the application of equations (45) and (49), consider the energy changes that occur when a horizontal stope is excavated ahead of a vertical fault, as shown in Fig. 4. This example will also serve to illustrate the analysis of energy changes that arise when a fault and stope intersect and, in particular, how the intersection mechanism can enhance the released energy and the volume of stope closure. The following three steps are evaluated.

A: Create the horizontal stope AB shown in Fig. 4.
B: Allow the fault plane PQ ahead of the stope to slip.
C: Advance the stope up to the fault plane and allow further fault slip to occur.

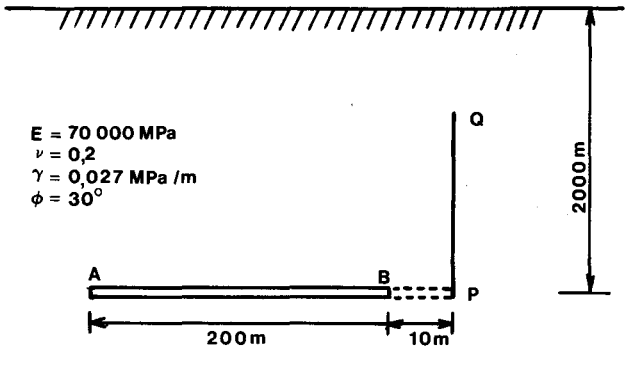

Fig. 4—Horizontal stope approaching a vertical fault plane

The values of the excess shear stress, τ_e, at the end of step A are shown as a function of distance along the weak plane from point P towards point Q in Fig. 5. The peak excess shear stress is just below 9 MPa. In step B, the plane is allowed to slip and the ride profile shown in Fig. 5 results, extending over a distance into the hangingwall of approximately 160 m compared with the extent of positive excess shear stress of about 105 m. The energy changes that occur at each stage are summarized in Table II. The rows A, B, B', and C in Table II represent total energy changes from the virgin state, v, to the current stage, whereas rows B–A, B'–A and C–B represent the relevant energy increments between stages. For example, the total available energy, given by equation (45), is 27 MJ/m, representing an increase from 1248,9 MJ/m in step A to 1275,9 MJ/m in step B. Deducting the work absorbed by friction sliding of 21,2 MJ/m yields a net unaccounted energy release of 5,8 MJ/m.

It is also interesting to note from Table II that the internal strain energy, ΔU, increases from step A to step B by the same amount (5,8 MJ/m^2) as the net released energy. In step A itself, ΔU should be equal to ΔW_A but differs owing to independent rounding errors encountered in the numerical evaluation of equations (44) and (45) respectively. (It is found that ΔU is more strongly affected by the solution accuracy than ΔW_A.)

Step B' illustrates the energy changes that occur if the stope closure is 'frozen' in step A. (The stope could be considered to be filled with incompressible material.) If the fault slip is then triggered, the total energy released is 23,2 MJ/m, of which 18,4 MJ/m is absorbed by sliding, giving an unaccounted released energy of 4,8 MJ/m. It is apparent that the change in volume of stope closure is, in this case, not instrumental in determining the net released energy. Indeed, it can be seen that the internal strain energy drops by an amount exactly equal to the total released energy (23,2 MJ/m), and that no additional energy is supplied by the body forces ($W^B - W^A = 0$).

Finally, it is of interest to examine the energy changes that occur when the stope is advanced up to the fault (step C). In that case, substantial additional stope closure and fault ride occur, with a correspondingly large change in the unaccounted released energy of 352 MJ/m. The fault–stope intersection can obviously have a major impact on the estimated magnitude of a seismic event.

To emphasize this point, the ride profile on the fault at the end of step C is plotted in Fig. 6 and is contrasted with the ride existing at the end of step B. The enormous release of energy associated with step C is due to the intersection of the fault with the stope, which enhances both the magnitude of fault slip and the volume of stope closure. This is an important consideration in the back analysis of large mining-induced seismic events[14], and may also be an important mechanism in the generation of seismic signals with 'implosional' focal mechanisms[15].

Energy Released by an Incrementally Advancing Stope

In previous analyses of the energy released in tabular mine layouts, it has been inferred that mining in small steps in a perfectly elastic medium is an aseismic process since the released energy is contained in the mined material[3]. However, no statement can be made using these arguments about the level of energy released in in-

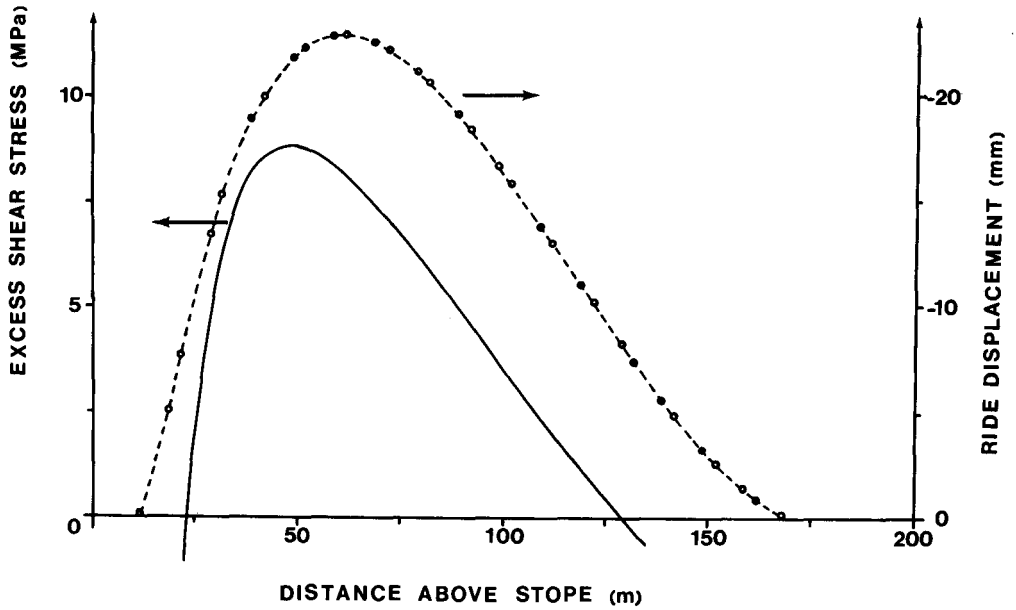

Fig. 5—Profiles of excess shear stress (solid line) and ride displacement (broken line) on a vertical fault plane 10 m ahead of a 200 m horizontal stope

TABLE II
ENERGY CHANGES BEFORE AND AFTER SLIP ON A VERTICAL FAULT LOCATED AHEAD OF A HORIZONTAL STOPE

Step no.	Volume of stope closure m^3/m	Volume of stope ride m^3/m	Volume of fault ride m^3/m	Change in internal strain energy (ΔU) MJ/m	Total energy available (ΔW_A) MJ/m	Energy absorbed by sliding (ΔW_D) MJ/m	Unaccounted energy released (ΔW_R) MJ/m	Inferred energy supplied (ΔW) MJ/m
A	46,4	0	0	1248,8	1248,9	0	1248,9	2497,7
B	46,9	−0,35	−2,2	1254,6	1275,9	21,2	1254,7	2530,5
B-A	0,6	−0,35	−2,2	5,8	27,0	21,2	5,8	32,8
B'	46,3	0	−1,9	1255,6	1272,1	18,4	1253,7	2497,7
B'-A	0	0	−1,9	−23,2	23,2	18,4	4,8	0
C	63,8	−1,14	−24,4	1605,5	1842,1	235,4	1606,7	3447,6
C-B	16,9	−0,79	−22,2	350,9	566,2	214,2	352,0	917,1

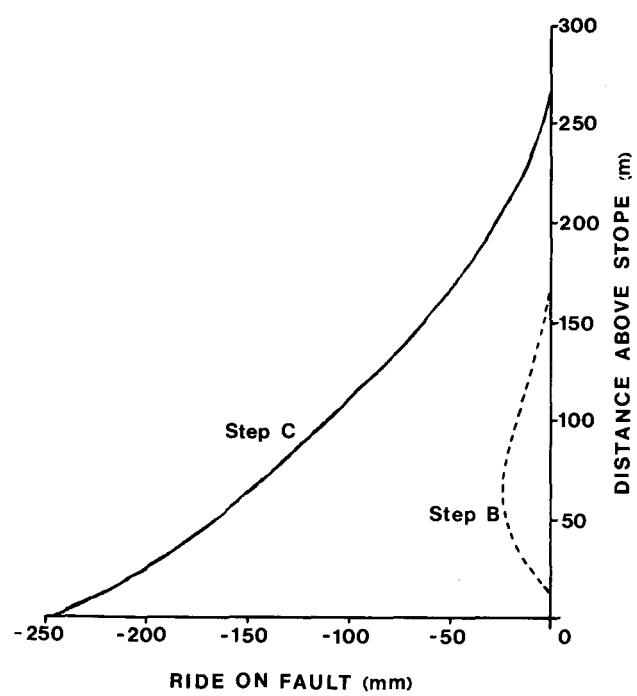

Fig. 6—Analysis of ride on a vertical fault plane intersecting a horizontal stope

elastic ground where off-reef fracturing does, in fact, occur. The method of analysis presented in this paper allows some insight to be gained into the release of energy if the stope-fracture zone can be represented as a specific pattern of discontinuities. In particular, consider the energy release accompanying incremental changes in the span of a parallel-sided panel in which vertical fracturing is allowed to occur at the stope faces. The specific geometry studied is shown in Fig. 7.

Ride on the vertical fractures is observed to occur in the sense shown in Fig. 7. Two sets of analyses were carried out with friction angles on the vertical fractures set to 30 and 50 degrees respectively, and with the cohesion on the fractures set to zero. In each analysis, the half-span of the panel was advanced by 10 m in five mining steps up to a half-span of 50 m. The released energy and the energy absorbed by frictional sliding are summarized for each mining step in Table III. The theoretical energy release for a horizontal parallel-sided panel of span s, without closure, is evaluated from equations (19) and (21) to be

$$W'_A = \pi(1 - \nu^2)(Q_z)^2 s^2/4E \text{ MJ/m}. \quad \ldots\ldots\ldots\ldots (55)$$

Substitution of the parameters in Fig. 7 shows the energy released per unit length of face for a panel of span

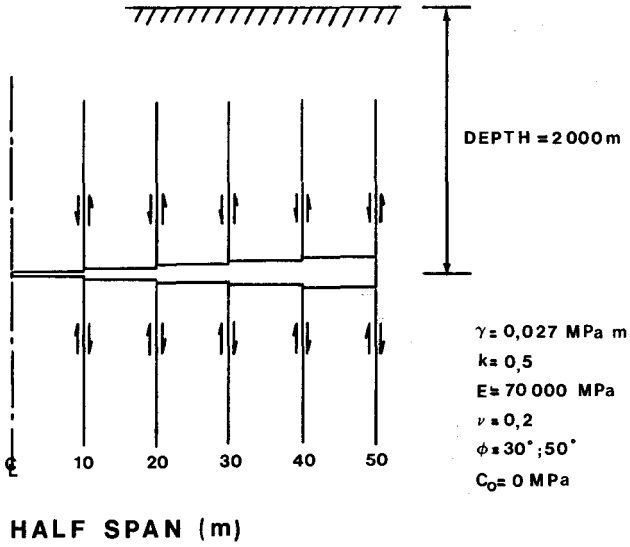

Fig. 7—Panel half-span changed in increments of 10 m with vertical fractures introduced at the edges of the panel in each increment

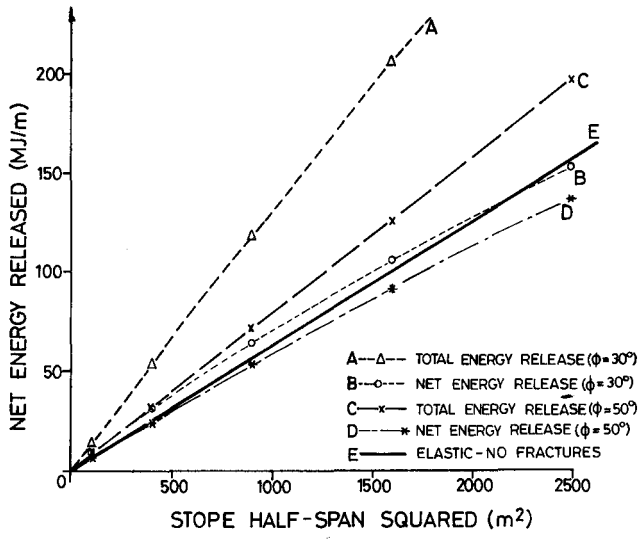

Fig. 8—Comparison of total and net energy released in a stope after the deduction of friction work for friction angles of 30 and 50 degrees on fractures at the stope face

s = 100 m to be 314,1 MJ/m or 157,0 MJ/m on each side of the panel, compared with the numerically computed value of 156,1 MJ/m shown as the last entry in the last column of Table III.

The values of cumulative energy released and net energy released, after deduction of the work done against frictional sliding, are plotted in Fig. 8 for comparison against the cumulative energy released when no sliding is allowed—equation (55). For example, with the friction angle equal to 30 degrees, line A represents the cumulative available energy on one side of the panel. Line B represents the net released energy after deduction of the energy absorbed by work against frictional sliding on the fractures, and can be seen to be remarkably close to the cumulative energy released for the 'elastic' case (line E), where no vertical fractures are allowed. When greater sliding resistance is introduced (friction angle = 50 degrees), the cumulative available energy decreases from line A to line C, and the net energy released (line D) is somewhat lower than the 'elastic' case (line E). As the friction angle is increased further, line D must tend towards line E, corresponding to a total suppression of sliding. It is apparent that, although sliding on the fracture planes absorbs a significant amount of energy, the overall level of available energy is also increased owing to increased stope closure. The net released energy is determined by the specific discontinuity pattern representing the fracture zone and the corresponding constitutive properties of the discontinuities.

It is of interest to re-evaluate the fracture-zone model shown in Fig. 7 with mining steps of different sizes. It is found that, when the cohesion is zero, the net unaccounted energy can be expressed in the form

$$W_R^t = g^2 f(n), \quad \ldots\ldots (56)$$

where g = size of mining step
n = number of mining steps.

When the logarithms of the net energy released values, reported in Table III for friction angles of 30 and 50 degrees, are plotted against the logarithms of the mining step number, it can be inferred that the function $f(n)$ in equation (56) is bounded by

$$f(n) < kn^{2-\epsilon}, \quad \ldots\ldots (57)$$

where k and ϵ are positive constants and $\epsilon < 0{,}2$.

For a fixed half span, λ, the step size and number of mining steps are related by

TABLE III
ENERGY CHANGES ACCOMPANYING THE INCREMENTAL MINING OF A PARALLEL-SIDED PANEL

	Friction = 30°, dilation = 0°				Friction = 50°, dilation = 0°				Elastic
Half-span m	Incremental work absorbed by sliding MJ/m	Cumulative sliding work MJ/m	Cumulative available energy MJ/m	Net energy released MJ/m	Incremental work absorbed by sliding MJ/m	Cumulative sliding work MJ/m	Cumulative available energy MJ/m	Net energy released MJ/m	Cumulative energy released MJ/m
10	4,8	4,8	13,8	9,0	1,5	1,5	8,1	6,6	6,2
20	17,1	21,9	53,5	31,6	4,7	6,2	30,3	24,1	24,9
30	31,7	53,6	117,8	64,2	11,0	17,2	70,4	53,2	56,1
40	47,7	101,3	206,2	104,9	17,5	34,7	125,4	90,7	99,8
50	64,7	166,0	318,6	152,6	25,1	59,8	196,2	136,4	156,1

Theoretical energy release = 157,0 MJ/m

$$\lambda = ng. \quad \text{..... (58)}$$

When equations (58) and (57) are substituted into equation (56), the net released energy is estimated to be

$$W_R^1 < k\lambda^2 n^{2-\epsilon}/n^2 = k\lambda^2/n^\epsilon. \quad \text{..... (59)}$$

In the limit, as $n \to \infty$, $W_R^1 \to 0$ provided $\epsilon > 0$.

However, it must be noted that, with $\epsilon < 0{,}2$, this limit is approached very slowly. If, for example, the length of the mining step is reduced from 10 m to 1 m in Fig. 7, the cumulative energy released will not be reduced by more than $1 - 10^{-0,2}$ or 37 per cent. The scaling relationship implied by equation (59) relates to the model shown in Fig. 7 with zero cohesion and will not be generally valid. Further investigation is required to elucidate the bounds on the unaccounted energy released for different fracture-zone models.

It is also of interest to compare the 'volume' of ride generated on the vertical fractures with the volume of stope closure, as a function of the stope half-span. This is displayed in Fig. 9, indicating a strongly non-linear influence of the angle of friction. When the friction angle is 30 degrees, the ride volume (line A) exceeds the closure volume (line B); however, when the friction angle is 50 degrees, the ride volume (line C) is much lower than the stope closure volume (line D). Although the volume of ride and the volume of closure are correlated in both cases, the proportions are considerably different. This has important implications in attempts to correlate stope closure with the off-reef seismicity that may be induced by off-reef deformations corresponding to localized shear mechanisms[16].

Conclusions

The following conclusions can be formulated.

(i) The simple unified method for the estimation of energy changes on multiple interacting fractures and tabular stopes presented here can readily be incorporated in stress-analysis programs based on the displacement-discontinuity method. In addition, relationships between 'axial' and 'transverse' energy release for plane-strain mine layouts can readily be derived.

(ii) The magnitudes of seismic events associated with fault movements can be seriously under-estimated if fault–stope intersection is not considered. The fault–stope intersection mechanism can enhance both the slip on the intersecting discontinuity and the stope closure. This may be manifested as an implosional focal mechanism in some seismic events.

(iii) The energy released in an incrementally advancing stope is affected by off-reef fracturing in a complicated manner. The net energy release after the work absorbed by frictional sliding has been deducted is not necessarily less than the energy release that would be computed if no fracturing occurred. The unaccounted component of released energy in a stope-face advance depends on the specific geometrical configuration of the fracture zone, which may change with each mining step. Mining in small but finite-sized steps is not necessarily aseismic.

(iv) The volume of ride on off-reef vertical fractures may correlate with the volume of stope closure, but the proportionality depends on the effective sliding resistance of the fractures and could be different in different geological environments.

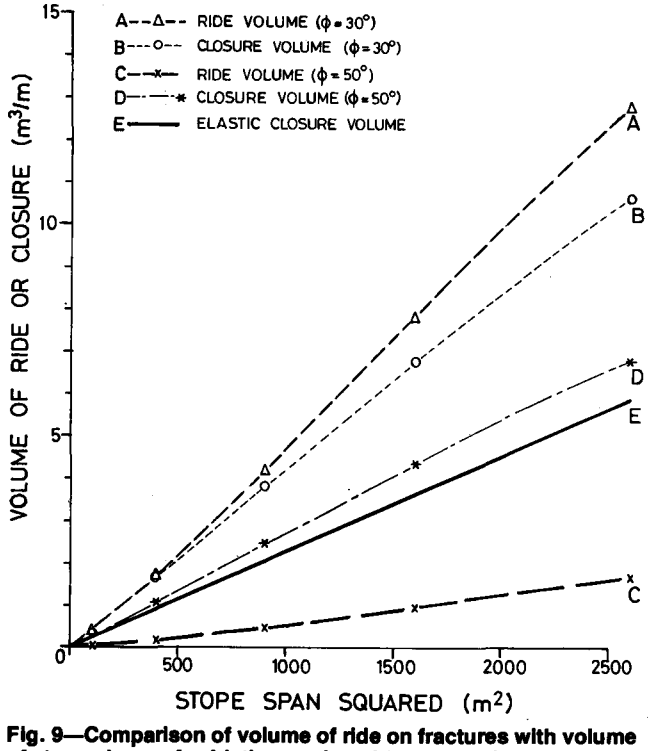

Fig. 9—Comparison of volume of ride on fractures with volume of stope closure for friction angles of 30 and 50 degrees on the fractures

Addendum

Consider a body bounded by an external surface S_e and containing internal 'discontinuity' surfaces. Each discontinuity is considered to have two sides that occupy the same spatial positions, initially, of a common surface denoted by S_d. A normal, with components n_i, is assigned to the surface S_d. The two sides of the discontinuity are then defined according to the direction of the assigned normal as shown in Fig. A1.

The surface on the side corresponding to the positive direction of the assigned normal is denoted S_d^+, and has

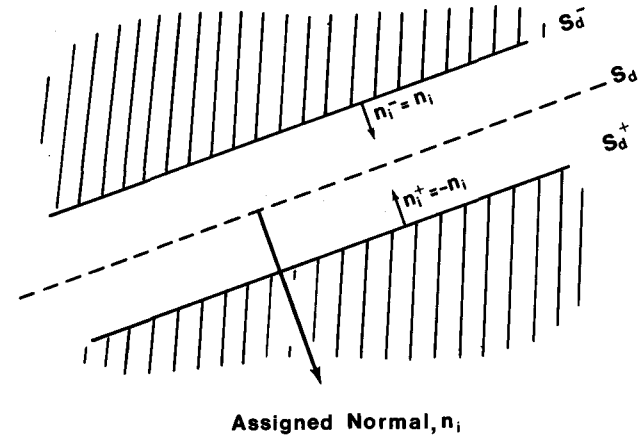

Fig. A1—Representation of two sides of a discontinuity surface having an assigned normal

an outward normal with respect to the neighbouring solid region of $[n_i^+] = -[n_i]$. The surface on the opposite side is denoted as S_d^- and has an outward normal, $[n_i^-] = [n_i]$. The jump in the displacement vector ('displacement discontinuity') when moving across the discontinuity surface is defined as

$$D_i = u_i^- - u_i^+, \quad \text{(A1)}$$

where u_i^- and u_i^+ are the components of the displacement vector at opposite points on the surfaces S_d^- and S_d^+ respectively. The body is now analysed in two states.

The first or 'virgin' state is obtained by the introduction of body forces F_i^v throughout the volume V and tractions T_i^v on the external surface S_e and the discontinuity surfaces S_d^- and S_d^+, such that the entire body remains in equilibrium and that no relative movement is permitted on the discontinuity surfaces. ($D_i = 0$ at all points of S_d.) The state of stress in the body is thus identical to that which would obtain if no discontinuities were present. This is illustrated in (a) of Fig. A2.

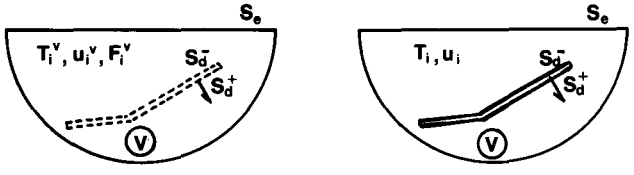

a) VIRGIN STATE b) INDUCED STATE

Fig. A2—Two states of an elastic body: a) the 'virgin' state with tractions, T_i^v, displacements, u_i^v, and body forces, F_i^v; and b) the 'induced' state with tractions, T_i, and displacements, u_i

The second state is determined as follows. The holding tractions on the discontinuity surfaces S_d^+ and S_d^- are adjusted in some specified and, in general, path-dependent sequence. The resulting state of the body is given in terms of total or terminal tractions T_i^t and displacements u_i^t. Body forces F_i^V remain unchanged. The second or 'induced' state is defined as the difference between the total and the virgin tractions and displacements. The induced tractions, T_i, and induced displacements, u_i, are therefore given by

$$T_i = T_i^t - T_i^v. \quad \text{(A2)}$$

and

$$u_i = u_i^t - u_i^v. \quad \text{(A3)}$$

respectively. It should be noted that no body forces exist in the 'induced' state, which is illustrated in (b) of Fig. A2.

Application of the Reciprocal Theorem[17] to the 'virgin' and 'induced' states yields the following expression:

$$\int_V F_i^v u_i \, dV + \int_S T_i^v u_i \, dS = \int_S T_i u_i^v \, dS, \quad \text{(A4)}$$

where $S = S_e + S_d^- + S_d^+$. (A5)

In going from the virgin to the final state, it is recognized that the body forces, F_i^v within V and initial tractions T_i^v on the external surface S_e will perform work on the body. This work is defined as W and is given by

$$W = \int_V F_i^v u_i \, dV + \int_{S_e} T_i^v u_i \, dS. \quad \text{(A6)}$$

Let U^v and U^t denote the total internal strain energy in the virgin and the final equilibrium states of the body, respectively. For an elastic body in a state of equilibrium, Clapeyron's theorem[17] asserts that

$$U^t = \tfrac{1}{2}\int_V F_i^t u_i^t \, dV + \tfrac{1}{2}\int_S T_i^t u_i^t \, dS$$

and

$$U^v = \tfrac{1}{2}\int_V F_i^v u_i^v \, dV + \tfrac{1}{2}\int_S T_i^v u_i^v \, dS.$$

Subtracting U^v from U^t and employing equations (A2) and (A3), together with the condition $F_i^v = F_i^t$, yields

$$U^t - U^v = \tfrac{1}{2}\int_V F_i^v u_i \, dV + \tfrac{1}{2}\int_S (T_i^v u_i + T_i u_i^v + T_i u_i) \, dS. \quad \text{(A7)}$$

Surface integrals are taken over $S_e + S_d^- + S_d^+$. In particular, consider a typical integral of the following form:

$$\int_{S_d^- + S_d^+} T_i u_i \, dS = \int_{S_d^-} \tau_{ij}^- n_j \bar{u}_i \, dS + \int_{S_d^+} \tau_{ij}^+ n_j^+ u_i^+ \, dS. \quad \text{(A8)}$$

Defining $D_i = u_i^- - u_i^+$ and noting that $n_i = n_i^- = -n_i^+$ and that $\tau_{ij}^- n_j = \tau_{ij}^+ n_j = T_i$, equation (A8) becomes

$$\int_{S_d^- + S_d^+} T_i u_i \, dS = \int_{S_d} T_i (u_i^- - u_i^+) \, dS = \int_{S_d} T_i D_i \, dS, \quad \text{(A9)}$$

where it is recognized that S_d^- and S_d^+ occupy the same spatial positions as S_d. On the external surface, S_e, it can be assumed that the induced stress, $T_i = 0$ or, on fixed portions of S_e, that the induced displacement, $u_i = 0$. Equation (A7) can then be written as

$$U^t - U^v = \tfrac{1}{2}\int_V F_i^v u_i \, dV + \tfrac{1}{2}\int_{S_e} T_i^v u_i \, dS + \tfrac{1}{2}\int_{S_d} T_i^t D_i \, dS, \quad \text{(A10)}$$

where $T_i^t = T_i^v + T_i$ and, from the nature of the postulated virgin-stress state, $u_i^{v-} - u_i^{v+} = D_i^v = 0$ on surfaces S_d. Similarly, equation (A4) can be written as

$$\int_V F_i^v u_i \, dV + \int_{S_e} T_i^v u_i \, dS + \int_{S_d} T_i^v D_i \, dS = \int_{S_e} T_i u_i^v \, dS. \quad \text{(A11)}$$

On the exterior surface S_e, the induced tractions, T_i are zero, or the virgin displacements, u_i^v, are zero on fixed parts of the boundary. The volume integral becomes

$$\int_V F_i^v u_i \, dV = \int_{S_e} T_i^v u_i \, dS - \int_{S_d} T_i^v D_i \, dS. \quad \text{(A12)}$$

Substitution of (A12) into equation (A6) yields

$$W = -\int_{S_d} T_i^v D_i \, dS. \quad \text{(A13)}$$

Similarly, substitution of (A11) into (A10) gives the following expression for the change in internal strain energy:

$$U^t - U^v = \tfrac{1}{2}\int_{S_d} T_i D_i \, dS. \quad \text{(A14)}$$

If the difference between the work done on the body, W, and the change in internal strain energy, $U^t - U^v$, are defined as the available energy, W_A,

$$W_A = W - (U^t - U^v). \quad \text{(A15)}$$

When equations (A13) and (A14) are combined,

$$W_A = -\tfrac{1}{2}\int_{S_d}(T_i^v + T_i^t)\, D_i\, dS. \quad \text{(A16)}$$

To determine energy expressions corresponding to an incremental change from a primitive state, p, which is different from the virgin state, v, to a final state, t, the incremental tractions, ΔT_i, displacements, Δu_i, and displacement discontinuities, ΔD_i, are defined as follows.

$$\Delta T_i = T_i^t - T_i^p \quad \text{(A17)}$$

$$\Delta u_i = u_i^t - u_i^p \quad \text{(A18)}$$

$$\Delta D_i = D_i^t - D_i^p. \quad \text{(A19)}$$

In state p and state t, the body force F_i^v remains fixed. Since the incremental tractions and displacements defined by equations (A17) to (A19) correspond to an equilibrium system, the reciprocal theorem[17] can be applied to the incremental system and the primitive system, p, to yield

$$\int_V F_i^v\, \Delta u_i\, dV + \int_S T_i^p\, \Delta u_i\, dS = \int_S \Delta T_i\, u_i^p\, dS, \quad \text{(A20)}$$

where $S = S_e + S_d$.

It should be noted that the discontinuity surfaces, S_d, cover all discontinuity positions up to the final state, t, including incremental changes occurring between state p and state t.

It is assumed that, on the 'external' surface, S_e, the total traction T_i^p is equal to a fixed value T_i^v or that the displacement is zero. This implies that, on S_e, ΔT_i is zero or that $u_i^p = 0$. Equation (A20) can therefore be written in the form

$$\int_V F_i^v\, \Delta u_i\, dV + \int_{S_e} T_i^v\, \Delta u_i\, dS + \int_{S_d} T_i^p\, \Delta D_i\, dS = \int_{S_d} \Delta T_i\, D_i^p\, dS. \quad \text{(A21)}$$

If the incremental work, ΔW, done on the system by the fixed surface and body forces is defined by

$$\Delta W = \int_V F_i^v\, \Delta u_i\, dV + \int_{S_e} T_i^v\, \Delta u_i\, dS, \quad \text{(A22)}$$

and (A22) is combined with (A21),

$$\Delta W = \int_{S_d} [\Delta T_i D_i^p - T_i^p\, \Delta D_i]\, dS. \quad \text{(A23)}$$

From the definitions (A17) and (A19), this can also be written as

$$\Delta W = \int_{S_d} [T_i^t D_i^p - T_i^p D_i^t]\, dS. \quad \text{(A24)}$$

When Clapeyron's theorem[17] is applied to the primitive state, p, and the final state, t, expressions are provided for the elastic strain energy of the form

$$2U^p = \int_V F_i^v u_i^p\, dV + \int_{S_e} T_i^p u_i^p\, dS + \int_{S_d} T_i^p D_i^p\, dS$$

$$2U^t = \int_V F_i^v u_i^t\, dV + \int_{S_e} T_i^t u_i^t\, dS + \int_{S_d} T_i^t D_i^t\, dS.$$

Subtracting U^p from U^t and making use of the postulate that on S_e the tractions are fixed and equal to T_i^v, or that the displacements are fixed, provides the relationship

$$2(U^t - U^p) = \Delta W + \int_{S_d} [T_i^t D_i^t - T_i^p D_i^p]\, dS,$$

where the definition (A22) of ΔW has been used. Substituting for ΔW from (A24) and defining $\Delta U = U^t - U^p$ result in the following expression for the incremental change in the internal strain energy:

$$\Delta U = \tfrac{1}{2}\int_{S_d}(T_i^t - T_i^p)\,(D_i^t + D_i^p)\, dS \quad \text{(A25)}$$

or

$$\Delta U = \tfrac{1}{2}\int_{S_d} \Delta T_i (D_i^t + D_i^p)\, dS. \quad \text{(A26)}$$

The available energy increment that must be dissipated is defined as

$$\Delta W_A = \Delta W - \Delta U. \quad \text{(A27)}$$

Substituting from equations (A24) and (A26), this can be written explicitly as

$$\Delta W_A = -\tfrac{1}{2}\int_{S_d}(T_i^p + T_i^t)\,(D_i^t - D_i^p)\, dS \quad \text{(A28)}$$

or

$$\Delta W_A = -\tfrac{1}{2}\int_{S_d}(T_i^p + T_i^t)\, \Delta D_i\, dS. \quad \text{(A29)}$$

In the particular case where the primitive state corresponds to the virgin stress state in which no discontinuities are mobilized, it is apparent that $T_i^p = T_i^v$ and that $D_i^p = 0$. Substituting these values into equations (A24), (A25), and (A28) recovers the total energy expressions (A13), (A14), and (A16) derived for the transition from the virgin state. The expressions for the total energy changes and the incremental energy changes are summarized in Table I in the main text.

It can be noted that, if part of the discontinuity surface, S_d^p, corresponds to the primitive state in which zero tractions act on S_d^p (i.e. open excavations) and that, if an extension ΔS_d is made to S_d^p such that the final traction over the new surface is zero, equation (A29) becomes

$$\Delta W_A = -\tfrac{1}{2}\int_{\Delta S_d} T_i^p D_i^t\, dS, \quad \text{(A30)}$$

which corresponds to the previous derivations of energy released for an open stope[2,12].

It is also of interest to note that alternative expressions for the incremental changes can be obtained by applying the expressions for the total energy change independently to the state p and the state t and subtracting the results. For example, the available energy in states p and t can be obtained from equation (A16) as

$$W_A^p = -\tfrac{1}{2}\int_{S_d}(T_i^v + T_i^p)\, D_i^p\, dS \quad \text{(A31)}$$

and

$$W_A^t = -\tfrac{1}{2}\int_{S_d}(T_i^v + T_i^t)\, D_i^t\, dS. \quad \text{(A32)}$$

If W_A^p is subtracted from W_A^t and the difference is equated to the right-hand side of equation (A28),

$$\int_{S_d}(T_i^t - T_i^v)\, D_i^p\, dS = \int_{S_d}(T_i^p - T_i^v)\, D_i^t\, dS, \quad \ldots \text{(A33)}$$

which is a reciprocal relationship that must hold between the induced stresses and the displacement discontinuities of the primitive and the final states.

Acknowledgements

The work described in this paper forms part of the research programme carried out by the Chamber of Mines Research Organization. Permission to publish these results is gratefully acknowledged. Grateful acknowledgement is also made to Drs N.C. Gay, J.A. Ryder, and P.A. Cundall for several useful comments and insights that they provided during the preparation of this paper.

References

1. SALAMON, M.D.G. Rock mechanics of underground excavations. *Advances in rock mechanics: Proceedings of the 3rd Congress, International Society for Rock Mechanics, Denver, Colorado.* Washington, National Academy of Sciences, 1974. vol. 1, Pt B, pp. 951–1099.
2. SALAMON, M.D.G. Rockburst hazard and the fight for its alleviation in South African gold mines. *Rockbursts: Prediction and control.* London, Institution of Mining and Metallurgy, 1983. pp. 11–36.
3. SALAMON, M.D.G. Energy considerations in rock mechanics: Fundamental results. *J. S. Afr. Inst. Min. Metall.*, vol. 84, no. 8. 1984. pp. 223–246.
4. WALSH, J.B. Energy changes due to mining. *Int. J. Rock Mech. Min. Sci. and Geomech. Abstr.*, vol. 14. 1977. pp. 25–33.
5. SAVAGE, J.C., and WALSH, J.B. Gravitational energy and faulting. *Bulletin of the Seismological Society of America*, vol. 68, no. 6. 1978. pp. 1613–1622.
6. AKI, K., and RICHARDS, P.G. *Quantitative seismology theory and methods.* San Francisco, W.H. Freeman & Company, 1980. vol. 1.
7. PIPER, P.S., and RYDER, J.A. An assessment of backfill for regional support in deep mines. *Backfill in South African mines.* Johannesburg, South African Institute of Mining and Metallurgy, 1988. pp. 111–136.
8. MALVERN, L.E. *Introduction to the mechanics of a continuous medium.* Englewood Cliffs, Prentice-Hall, 1969.
9. CROUCH, S.L., and STARFIELD, A.M. *Boundary element methods in solid mechanics.* London, George Allen & Unwin, 1983.
10. NAPIER, J.A.L., and STEPHANSEN, S.J. Analysis of deep-level mine design problems using the MINSIM-D boundary element program. *Proceedings of the 20th International Symposium on the Application of Computers and Mathematics in the Mineral Industries.* Johannesburg, South African Institute of Mining and Metallurgy, 1987. vol. 1, pp. 3–19.
11. SALAMON, M.D.G. Two-dimensional treatment of problems arising from mining tabular deposits in isotropic or transversely isotropic ground. *Int. J. Rock Mech. Min. Sci.*, vol. 5. 1968. pp. 159–185.
12. COOK, N.G.W., HOEK, E., PRETORIUS, J.P.G., ORTLEPP, W.D., and SALAMON, M.D.G. Rock mechanics applied to the study of rockbursts. *J. S. Afr. Inst. Min. Metall.*, vol. 66. 1966. pp. 435–528.
13. RYDER, J.A. Excess shear stress in the assessment of geologically hazardous situations. *J.S. Afr. Inst. Min. Metall.*, vol. 88, no. 1. 1988. pp. 27–39.
14. WEBBER, S.J. Numerical modelling of a repeated fault slip. *J. S. Afr. Inst. Min. Metall.*, vol. 90, no. 6. Jun. 1990. pp. 133–140.
15. WONG, I.G., and MCGARR, A. Implosional failure in mining-induced seismicity: A critical review. *2nd Seismicity in Mines Symposium.* University of Minnesota, 1988. pp. 13–28.
16. MCGARR, A. Seismic moment and volume changes. *J. Geophys. Res.*, vol. 81, no. 8. 1976.
17. SOKOLNIKOFF, I.S. *Mathematical theory of elasticity.* New York, McGraw-Hill, 2nd ed., 1956.

Gold Fields National Engineering Awards

The winners of the coveted Gold Fields National Engineering Awards were announced at a function held at the Gold Fields head office on Thursday, 7th March, 1991. Mr Robin Plumbridge, Chairman and Chief Executive Officer of Gold Fields, presented the awards.

The first prize of R10 000 was presented to Clive Wynne, final-year mechanical-engineering student at the University of Cape Town, for his final-year thesis on the fluidized-bed engine silencer and his oral presentation of the thesis.

On presenting the award, Mr Plumbridge referred to the long-overdue statutory changes transforming South African society, and said that these efforts would be futile unless that same dynamic was applied to the beneficiation of our most valuable, and as-yet unexploited natural resource—human potential.

Clive Wynne from UCT with his fluidized-bed engine silencer, for which he won first prize in the annual Gold Fields National Engineering Awards

In addition to walking off with the first prize, Mr Wynne won a total of R20 000 for his university. This makes the first prize worth a total of R30 000—Southern Africa's most sought-after academic prize in the field of engineering.

The Universities of Pretoria and the Witwatersrand tied for second place.

The remaining six candidates, who received R1000 each for having been nominated by their universities, are as follows, together with the titles of their theses:

C. Menyennett — RAU (Electrical)
Die Ontwerp van 'n Simpleks Basisbandmodem vir ISDN

R.G. Berndt — Wits (Aeronautical)
The Design, Construction and Testing of a Hypersonic Wind Tunnel

J. Louw — Stellenbosch (Chemical)
Ontwatering van Aseotrope Etanol deur Selektiewe Adsorpsie op Biomateriale

D. Proudfoot and P.E. van der Kouwe — Pretoria (Electrical)
Fibre Optic Gyroscope

E.J. Braithwaite — Natal (Civil)
Design Project 1990: Technology Exhibition Centre

R. van den Berg — Potchefstroom (Electrical)
Elektroniese Raakskakelaar

Cullinan awards

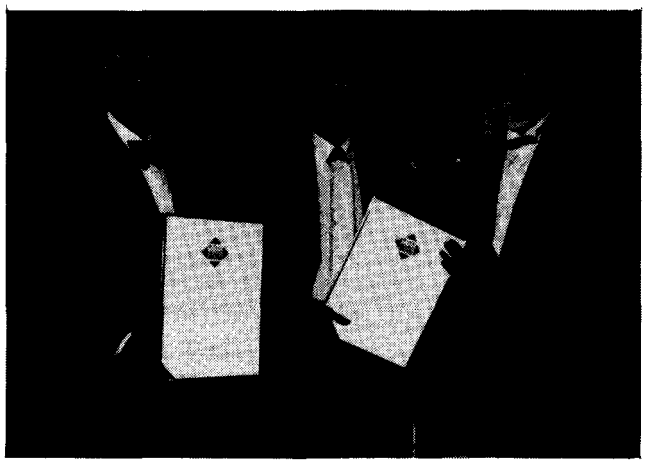

Mr Ken Ball (centre), Multotec Manufacturing Manager Research & Development, and Mr E.J. Holtz (left), Multotec Managing Director, receive a Cullinan Design Award for their Mato Belt Planer from guest speaker Dr Bob Blaich

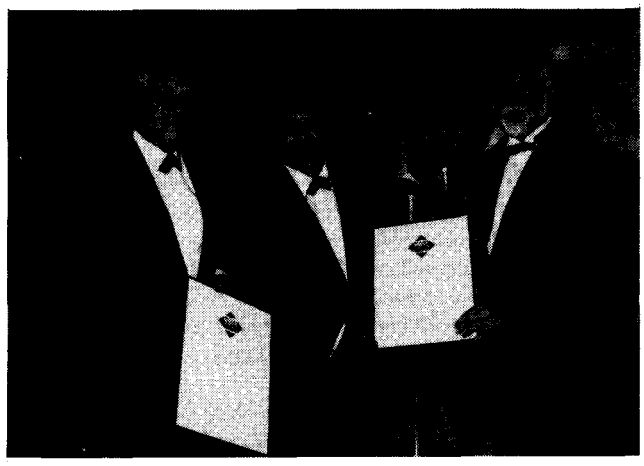

Mr Don Alexander (left) and Mr Steven Alexander (centre) of D & S Engineering receive a Cullinan Design Award for their mining product Abextra from guest speaker Dr Bob Blaich

Mr Paul McKelvey of New Consort Mining receives a Cullinan Design Award for their Safe-T-Pack from guest speaker Dr Bob Blaich

Pictured receiving the Chairman's Award are the makers of Packsetter: from left, Mike Faure, HLH; John Thorpe, Tufbag; Richard Wood, Nicro; Norman Cook, Tufbag; Jurgen Desit, Nicro; Prof. H.C. Viljoen, Chairman of the Cullinan Design Awards judging panel; Dr Rod Smart, Fosroc; Geoff Joubert, Fosroc; and Martin van der Merwe, HLH

* Released by Jimmy Thomas & Associates (Pty) Ltd, PO Box 782114, Sandton 2146.